

Poly(furfuryl alcohol) nanospheres: a facile synthesis approach based on confinement effect of polymer and a template for synthesis of metal oxide hollow nanospheres

WEI-ZHI WANG^{1,*}, ZHI-QIANG LI¹, KONG-LIN WU¹, YA-JING LU¹, YA-FEI XU¹ and XIN-JIE SONG²

¹The Key Laboratory of Functional Molecular Solids, Ministry of Education, Anhui Laboratory of Molecular-Based Materials, College of Chemistry and Materials Science, Anhui Normal University, Wuhu 241000, PR China

²Department of Food Science and Technology, Yeungnam University, Gyeongsan 712749, Republic of Korea

MS received 7 July 2015; accepted 10 August 2015

Abstract. This paper describes a facile hydrothermal approach to the large-scale synthesis of well-dispersed poly(furfuryl alcohol) (PFA) nanospheres with an average diameter of 350 nm in the presence of poly(vinyl pyrrolidone) (PVP). Scanning electron microscopy and transmission electron microscopy studies showed that different morphologies of PFA could be obtained by adjusting the ratio of PVP and furfuryl alcohol (FA). As a whole, the results demonstrate that PVP plays a key role in controlling the polymerization process of FA. The confinement effect of PVP is proposed to explain the formation process of PFA nanospheres. Furthermore, the as-prepared PFA nanospheres have a functional surface that allow them to act as an ideal template for fabricating metal oxide hollow nanospheres.

Keywords. Poly(furfuryl alcohol); nanospheres; hydrothermal; hollow.

1. Introduction

Furfuryl alcohol (FA) is a product derived from crop residues made by reducing furfural.¹ As a very reactive substance, it can form a black resin of poly(furfuryl alcohol) (PFA) through heated or acid-catalysed polymerization.^{2,3} FA is compatible with many organic polymers and inorganic materials,⁴ and it provides a high carbon yield when pyrolysed. Therefore, PFA is important for use in metal-casting molds, corrosion-resistant materials and negative photoresists.⁵ It has also been shown to act as a precursor to synthesize various carbon-based materials and polymer composites for a wide range of applications, such as adsorbents, separation membranes, electrodes of fuel cells, lithium batteries, electric double-layer capacitors, etc.⁶ Although there have been systematic studies on the polymerization mechanisms and condensation kinetics of PFA,^{7–9} little attention has been devoted to synthesize nanoscale PFA species, for example synthesis of PFA nanospheres. In recent years, the design and synthesis of polymer nanospheres has garnered the interest of researchers owing to their fundamental scientific importance and potential applications,¹⁰ including drug and DNA delivery and photonic band-gap crystal.¹¹ Many approaches for preparing polymer nanospheres have been developed, which can be summarized into three

categories according to the preparation method: (i) as a conventional preparation method, emulsion or microemulsion polymerization can make polymeric particles in the size range of 10–10³ nm.^{12,13} (ii) As a mimic of globular proteins, self-assembly of linear block copolymers has been used to prepare nanospheres with core–shell morphology.^{14,15} (iii) In recent times, a new method involving the collapse and intramolecular coupling of single-polymer chains to fabricate nanospheres has been proposed.^{16–18} Despite these advancements, it is still important and meaningful to explore convenient and facile methods to fabricate polymer nanospheres.

Hydrothermal process has been acknowledged as one of the most efficient methods for preparing inorganic nanomaterials with various morphologies.¹⁹ In this study, a facile polymer-assisted hydrothermal approach was employed to obtain well-dispersed PFA nanospheres. After investigating the effect factor on morphology of the products, a possible polymer confinement polymerization process was identified to explain the formation of PFA nanospheres. Since conventionally hydrothermal process can be used to prepare spherical PFA in nanoscale, it is believed that this is an effective approach because it is simple, low-cost and ideal for large-scale production of polymer nanospheres. Furthermore, the surface of as-prepared PFA nanospheres is functionalized, which offer a beneficial environment for interactions with metal cations and subsequent conversion to metal oxide hollow nanospheres through removal of the PFA core.

*Author for correspondence (wangwz@mail.ahnu.edu.cn)

2. Experimental

2.1 Preparation of PFA nanospheres

All reagents were of analytical grade (Shanghai Chemical Reagents Co.) and used without further purification. A typical procedure was as follows: an aqueous solution of 40 ml was first prepared by dissolving 1 g of poly(vinyl pyrrolidone) (PVP) (K30, polymerization degree = 360) in distilled water. Then, 0.5 ml of FA was added dropwise into the former solution with constant stirring until a homogeneous clear solution was formed. The resulting solution was transferred into a Teflon-lined stainless-steel autoclave. The autoclave was sealed and maintained at 160°C for 12 h. The red-brown products were isolated by centrifugation (7000 rpm, 8 min). Then, products were washed by cycles of dispersion/washing/centrifugation in distilled water and ethanol several times to remove excess PVP. Finally, the products were dried in a vacuum at 60°C for 6 h.

2.2 Preparation of α -Fe₂O₃ hollow nanospheres

A specific amount of as-prepared PFA nanospheres was well dispersed into 40 ml of water with the assistance of sonication for 10 min. FeCl₃·6H₂O (1 mmol) was dissolved into the above solution with vigorous stirring for 30 min; after which 3 ml of 1 M NaOH aqueous solution was slowly added into the mixture with stirring. The mixture was kept at room temperature for 5 h with vigorous stirring. The products were collected by centrifugation and cleaned by three cycles of centrifugation/washing/redispersion in water and ethanol before being dried at 60°C for 4 h. Finally, α -Fe₂O₃ hollow nanospheres were obtained after calcination at 500°C in static air for 2 h.

2.3 Characterization

Transmission electron microscopy (TEM) images of the as-prepared products were taken on a Hitachi H-800 TEM at an accelerating voltage of 200 kV. Morphologies of the products were also characterized using a scanning electron microscope (SEM, JEOL-6300F). Fourier transform infrared (FT-IR) spectrum was recorded on a Bruker EQUINOX55 FT-IR spectrometer using wavenumbers of 500–4000 cm⁻¹ at room temperature. The sample was pressed into disk with KBr. ¹H NMR spectrum was measured with a Bruker AVANCE 300 spectrometer at a frequency of 300 MHz. The products were dissolved in CDCl₃, and TMS was used as an internal reference.

3. Results and discussion

3.1 Morphology and characterization of PFA nanospheres

The morphology and size of the as-prepared products were examined by TEM and SEM. Figure 1a and b clearly

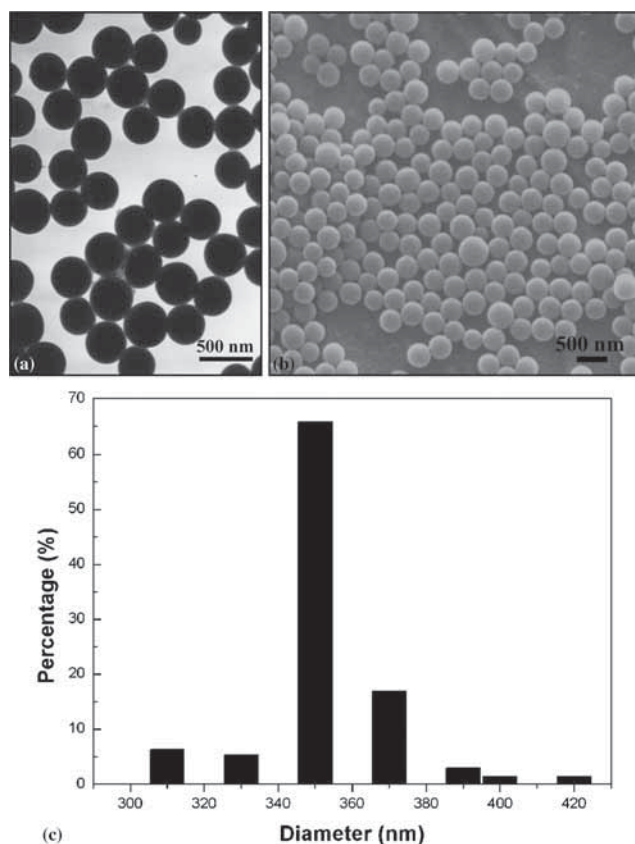


Figure 1. PFA nanospheres: (a) TEM and (b) SEM image. (c) Size distribution histogram of about 200 PFA nanospheres.

demonstrates that the products are composed of large quantities of nanospheres with very smooth surfaces and good dispersibility. Figure 1c shows a size distribution histogram of about 200 nanospheres from the SEM image, showing that these nanospheres have a narrow size distribution with an average diameter of 350 nm. The dispersity of the as-prepared nanospheres is reflected by the polydispersity index (PDI). The closer PDI is to 1, the more monodisperse the particles are.²⁰ PDI is defined by the following:^{20–22}

$$\text{PDI} = \frac{D_w}{D_n}, \quad D_w = \frac{\sum n_i D_i^4}{\sum n_i D_i^3}, \quad D_n = \frac{\sum n_i D_i}{\sum n_i}, \quad (1)$$

D_w is the weight average diameter, D_n the number average diameter and n_i the number of particles with diameter D_i . The PDI of the as-prepared products is about 1.007, which indicates that these nanospheres have good dispersibility.

Figure 2a shows the FT-IR spectrum of the nanospheres, confirming they are PFA. The bands at 733, 1016, 1162, 1505 and 3122 cm⁻¹ are attributed to stretching of the =C–O–C= and =C–H groups of the furan rings. The bands at 788 and 1563 cm⁻¹ are the result of bending out of the plane of the CH linkage and stretching of the –C=C– groups in the 2–5 disubstituted furan rings. The bands at 1357 and 1608 cm⁻¹ are because of the ring stretch modes of the two substituted furan rings. The aliphatic CH₂ groups in the polymer are responsible for the bands at 2920 and 1421 cm⁻¹,

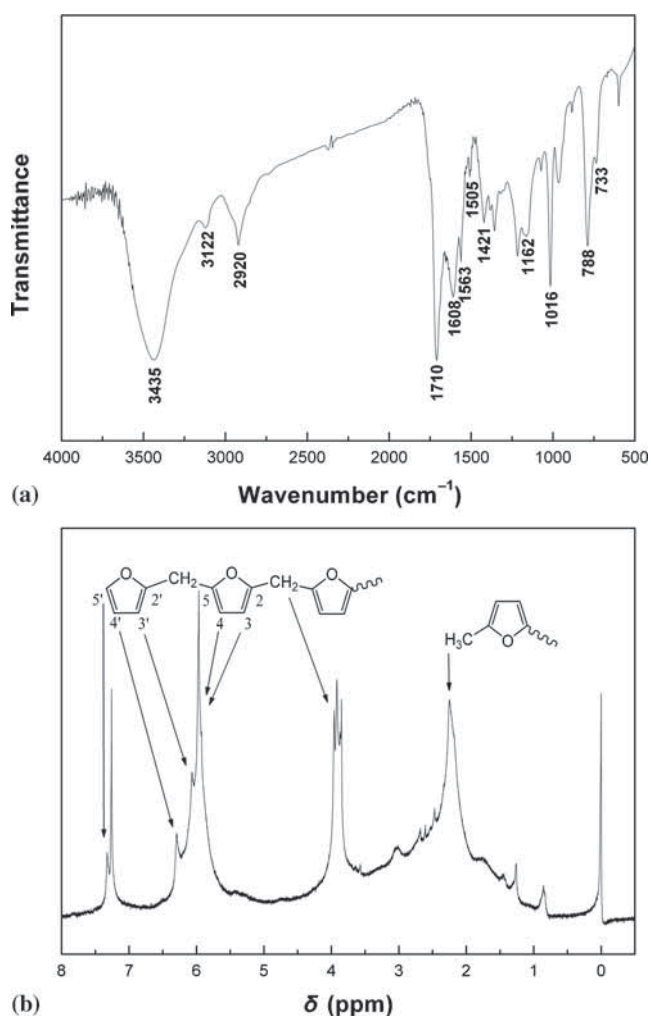


Figure 2. (a) FT-IR spectrum and (b) ^1H NMR spectrum (300 MHz, solvent: CDCl_3) of PFA nanospheres.

whereas the band at 3435 cm^{-1} is assigned to stretching of the OH end groups in PFA. The absorption band at 1710 cm^{-1} is ascribed to carbonylic structures originating from opening of some furan rings by electrophilic attack. These characteristic absorption bands are similar to bulk PFA resin in the literature.^{23–25} There are no characteristic vibrational absorption signals for the $\text{C}=\text{O}$ bond of PVP at $\sim 1665\text{ cm}^{-1}$ in the FT-IR spectrum,²⁶ indicating that PVP was completely removed by repeated washing with distilled water and absolute ethanol.

The ^1H NMR spectrum of the PFA nanospheres was also checked in order to understand the polymerization of FA (see figure 2b). The proton signal at 7.33 ppm corresponds to the terminal furan ring (H_5); signals between 5.80 and 6.40 ppm can be assigned to the protons H_3 and H_4 of the furan ring, in addition to those arising from H_3 (6.07 ppm) and H_4 (6.30 ppm). The complex signals centred around 3.90 ppm are due to the $-\text{CH}_2-$ groups joined to the C_2 and C_5 positions of the two furan rings. The broad signals around 2.2 ppm are assigned to $-\text{CH}_3$ end groups attached

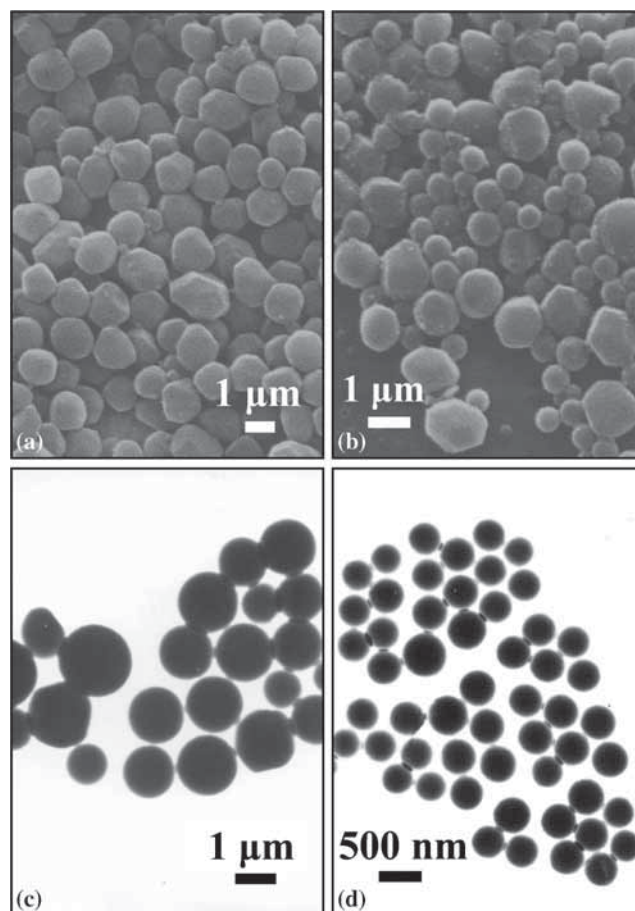
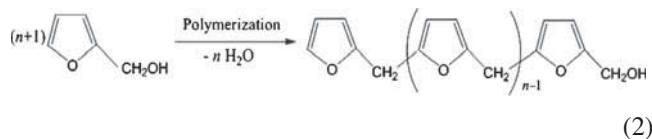


Figure 3. SEM and TEM images of PFA prepared with various ratios of PVP/FA (g ml^{-1}): (a) 0.4, (b) 0.5, (c) 1 and (d) 2.5.

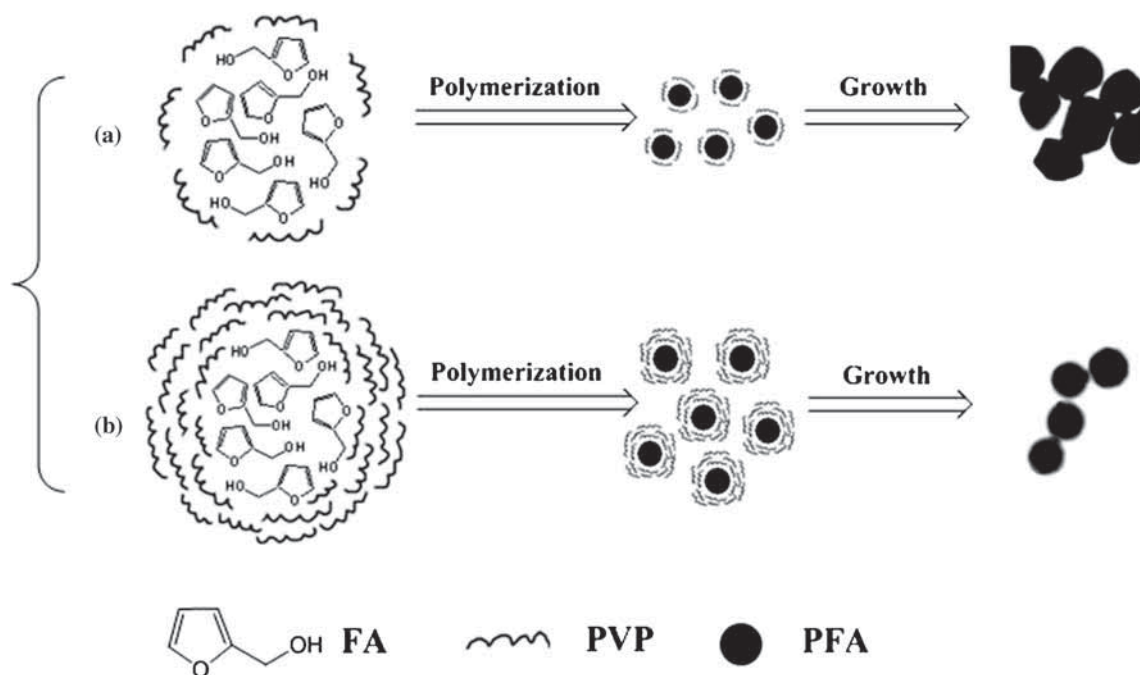
to the C_2 or C_5 position of the furan ring.²⁷ This is not new since methylated FA oligomers have been isolated and characterized previously.^{28,29} The signals between 1.50 and 3.50 ppm indicate the presence of other aliphatic protons.³⁰ The likely origin of the unassigned aliphatic signals is the opening of some furan rings.¹ No signal is observed around 4.50 ppm, indicating the absence of detectable amounts of $-\text{CH}_2-\text{O}-\text{CH}_2-$ bridges in these polymers.²⁴ Judging from the ^1H NMR spectrum, it can be concluded that the polymerization of FA mainly involves condensation of the OH group with the mobile hydrogen atom of the heterocycle at C_5 ,³¹ as indicated in equation (2).



The above analyses demonstrate that the spherical PFA nanomaterials were successfully formed by polymerization of FA under a facile hydrothermal process. Since neither expensive reagents nor organic solvents are used in the synthesis of polymer nanospheres, this approach is cheaper, greener and easier in comparison with other techniques.

Table 1. Morphology and size of PFA prepared using different ratios of PVP/FA.

PVP (g)	FA (ml)	Ratio = PVP/FA (g ml ⁻¹)	Morphology	Size
None	0.5	0	Bulk	—
0.1	0.5	0.2	Bulk	—
0.2	0.5	0.4	Polyhedron	1.5–2 μm
1	2	0.5	Polyhedron + sphere	0.5–1.5 μm
0.5	0.5	1	Sphere + polyhedron	0.5–1.2 μm
0.8	0.5	1.6	Sphere	~400 nm
1	0.5	2	Sphere	~350 nm
1	0.4	2.5	Sphere	~350 nm
4	1	4	Sphere	~400 nm
3	0.5	6	Sphere	~400 nm
1	0.1	10	Sphere	~280 nm

**Figure 4.** Schematic illustration of possible formation of PFA with different morphologies: (a) PVP is deficient and (b) PVP is excessive.

3.2 Effect of ratio of PVP/FA

In our experiment, PVP was shown to play a significant role in the formation of PFA nanospheres. When no PVP was added to our reaction system, no PFA nanospheres formed and only black bulk PFA resin was obtained. To understand the effect of PVP on polymerization of FA and the formation of PFA nanospheres, morphology and size of PFA were investigated using TEM and SEM under the same conditions except for different ratios of PVP/FA (g ml⁻¹).

At a low PVP/FA ratio (0.2), main products were mainly bulk PFA resin. Increasing the amount of PVP to a PVP/FA ratio of 0.4 resulted in reddish brown precipitates. SEM image (figure 3a) reveals that products were large polyhedrons with sizes of about 1.5–2 μm. After increasing the PVP/FA ratio to 0.5, PFA nanospheres formed, but

main products were still large polyhedrons (figure 3b). Further increasing the PVP/FA ratio to 1 also increased the proportion of PFA nanospheres (figure 3c). TEM image (figure 3d) shows that most of the products at a PVP/FA ratio of 2.5 were PFA nanospheres with an average diameter of 350 nm, which is similar to typical products (ratio of 2). These images clearly demonstrate that the morphology of PFA could be developed from a large polyhedron to small sphere by increasing the ratio of PVP/FA. The detailed relationship between the PVP/FA ratio and morphology and size of PFA is listed in table 1.

3.3 Possible formation process of PFA

Based on our above experimental results, it can be concluded that PVP/FA ratio is an important factor in the formation of

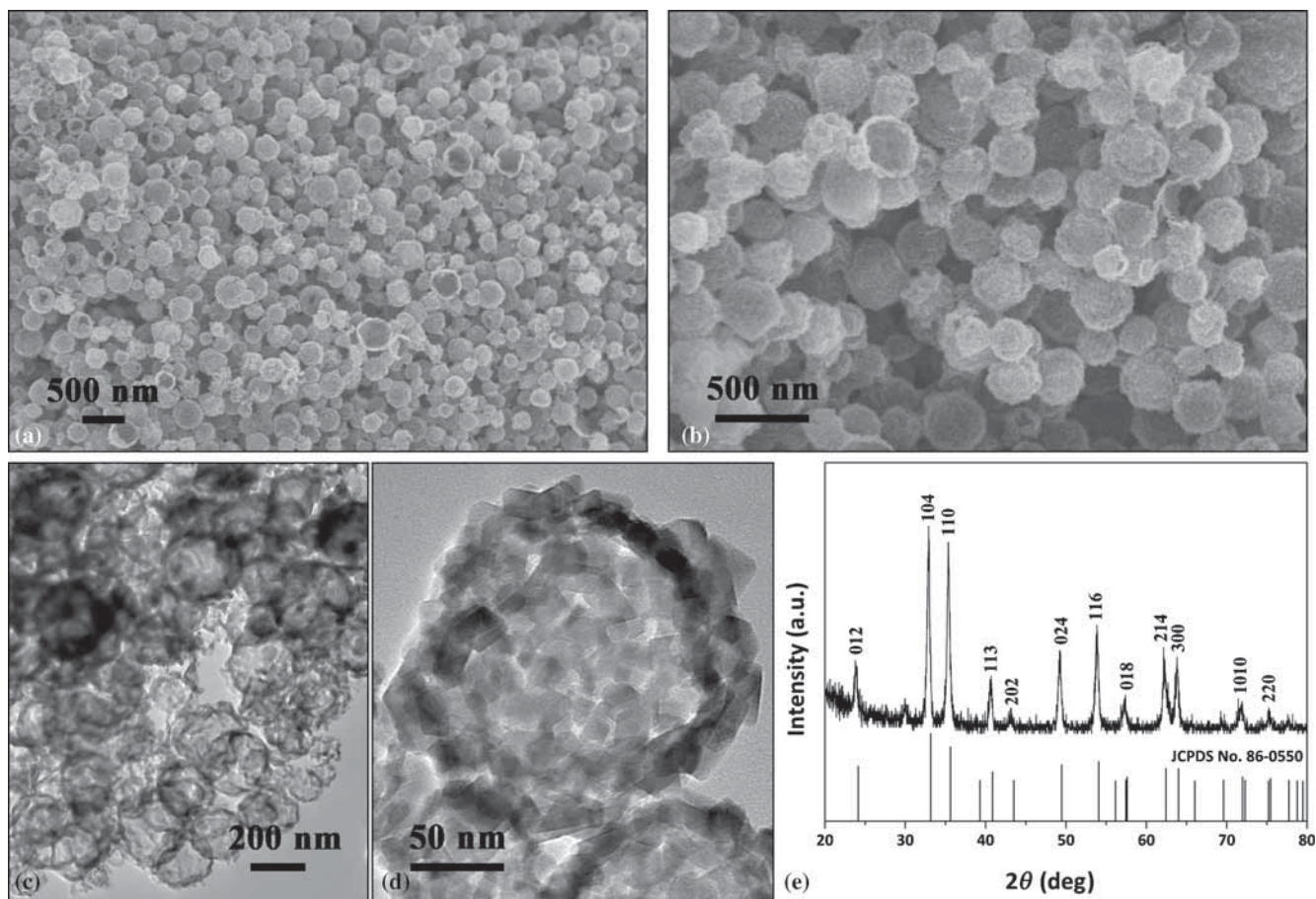


Figure 5. As-obtained α -Fe₂O₃ hollow nanospheres: (a) general and (b) magnified SEM image; (c) TEM and (d) magnified TEM image; and (e) XRD pattern.

PFA nanospheres with uniform diameter and good dispersibility. In former studies, PVP merely served as a steric stabilizer to synthesize spherical polymer with good dispersibility. Alteration of PVP concentration did not affect the spherical morphology of polymer.^{32–34} In our system, different morphologies of PFA could be obtained by adjusting the PVP/FA ratio. Therefore, it was speculated that PVP can be used not only as a colloidal stabilizer but also as a control agent in the formation of PFA. As reported, pyrrole rings of PVP participate in an organic–organic interaction with the furan rings of FA due to π – π stacking.³⁵ As a result of this interaction, PVP may have a confinement effect on controlling the polymerization of FA, resulting in the formation of PFA with different morphologies.

In our reaction system, FA monomer polymerizes to form bulk PFA resin without PVP. Upon PVP addition, polymerization of FA is restricted by PVP owing to the interaction between the pyrrole rings and furan rings. When there is a higher amount of FA than PVP (for example, PVP/FA ratio of 0.4), PVP cannot completely confine polymerization of FA, resulting in the formation of large polyhedral PFA. However, when the amount of PVP is excessive, polymerization of FA is controlled completely by PVP. Such strong confinement is responsible for the good spherical morphology

and dispersibility of products with uniform size. The above-mentioned formation process of PFA can be illustrated as in figure 4.

Based on the above discussion, it can be concluded that spherical PFA can be obtained as long as polymerization of FA is entirely confined by excessive PVP. For example, although the amount of FA in experiment No. 9 was higher than No. 3 (table 1), products were mainly small PFA nanospheres instead of large polyhedrons thanks to the confinement effect of PVP. Therefore, the formation of PFA nanospheres based on the confinement effect of PVP should be reasonable.

3.4 Characterization of α -Fe₂O₃ hollow nanospheres

PFA is often used as a precursor in preparing porous carbons or glassy carbons.⁶ Considering their functionalized surface and good dispersibility, our as-prepared PFA nanospheres are believed to be an ideal template for fabricating hollow nanostructures as well.³⁶ The surface of as-prepared PFA nanospheres contains a large quantity of functional groups such as –OH and –CH₂– according to a previous FT-IR study. The functional groups on the surface of PFA are able to bind to metal cations through electrostatic

interactions or coordination. In the subsequent calcinations process, the PFA core is removed, after which surface layers of metal cations are gradually densified to form oxide hollow nanospheres. The experimental result is in good agreement with our expectations. α -Fe₂O₃ hollow nanospheres can be obtained successfully on a large scale.

The general SEM image (figure 5a) of the products shows exclusively spherical structures with diameters ranging from 200 to 250 nm. The diameters of these nanospheres with rough surfaces are reduced to about 35% of the original diameters of the PFA nanospheres. As shown in the high-magnification SEM image (figure 5b), some broken spherical products can be observed, which shows the character of the hollow structure. This hollow structural character can be observed more clearly through TEM images of the products. TEM image (figure 5c) confirms that the hollow-sphere structure of as-obtained products have a shell wall thickness of about 20–30 nm. A high-magnification TEM image (figure 5d) shows that the shell is formed from packed nanoparticles, which is consistent with the rough surface observed in the SEM images. Figure 5e displays the XRD pattern of the hollow nanospheres. All diffraction peaks can be readily indexed to hexagonal α -Fe₂O₃ (JCPDS no. 86-0550), and sharpness of the peaks implies the high crystalline quality of the as-obtained sample.

As the functionalized surface of the as-prepared PFA nanospheres interacts with Fe³⁺ cations, an Fe(OH)₃ layer will form on the surface of the PFA nanospheres when NaOH solution is added to the reaction system. The PFA core can be removed and the Fe(OH)₃ layer decomposed during the calcination process, which will lead to the crystallization and condensation of α -Fe₂O₃, resulting in the formation of hollow nanospheres. This can explain the shrinkage of the diameter of α -Fe₂O₃ hollow nanospheres compared to that of PFA nanospheres. The formation process of α -Fe₂O₃ hollow nanospheres could be extended to the preparation of many other metal oxide hollow nanospheres, with further work following on.

4. Conclusions

In summary, a facile hydrothermal approach has been developed for the fabrication of PFA nanospheres with good dispersibility. The experimental results demonstrated that the PVP/FA ratio imposes a significant influence on PFA morphology. According to the experimental discussions and former reports, a possible formation process of PFA nanospheres based on the confinement effect of PVP was proposed. Owing to interactions between the pyrrole rings and furan rings, PVP molecule acts as a control agent to restrict polymerization of FA. PFA nanospheres can be obtained only when polymerization of FA is entirely confined by PVP. Due to the functionalized surface, the as-prepared PFA nanospheres are an ideal template for the fabrication of hollow nanospheres, such as successful synthesis of α -Fe₂O₃ hollow nanospheres. This feasible approach presents a

new paradigm for the preparations of well-dispersed polymer nanospheres and hollow nanospheres.

Acknowledgements

This work was financially supported by the National Natural Science Foundation of China (No. 21201008 and No. 21501004) and the Anhui Provincial Natural Science Foundation (No. 1208085QB31).

References

- Gandini A and Belgacem M N 1997 *Prog. Polym. Sci.* **22** 1203
- Gonzalez R, Martinez R and Ortiz P 1992 *Makromol. Chem.* **193** 1
- Magalhaes W L E and da Silva R R 2004 *J. Appl. Polym. Sci.* **91** 1763
- Kherroub D E, Belbachir M and Lamouri S 2015 *Bull. Mater. Sci.* **38** 57
- Sthel M, Rieumont J and Martinez R 1999 *Polym. Test.* **18** 47
- Wang H T and Yao J F 2006 *Ind. Eng. Chem. Res.* **45** 6393
- Gandini A and Martinez R 1983 *Makromol. Chem.* **184** 1189
- Pepper D C and Ryan B 1983 *Makromol. Chem.* **184** 395
- Gonzalez R, Rieumont J, Figueroa J M, Siller J and Gonzalez H 2002 *Eur. Polym. J.* **38** 281
- Ugelstad J, Stenstad P, Kilaas L, Prestvik W S, Rian A, Nustad K, Herje R and Berge A 1996 *Macromol. Symp.* **101** 491
- Johnson S A, Ollivier P J and Mallouk T E 1999 *Science* **283** 963
- Pavel F M 2004 *J. Dispersion Sci. Technol.* **25** 1
- Zhang G Z, Niu A Z, Peng S F, Jiang M, Tu Y F, Li M and Wu C 2001 *Acc. Chem. Res.* **34** 249
- Zhang Q, Remsen E E and Wooley K L 2000 *J. Am. Chem. Soc.* **122** 3642
- Butun V, Billingham N C and Armes S P 1998 *J. Am. Chem. Soc.* **120** 12135
- Antonietti M, Bremser W and Pakula T 1995 *Acta Polym.* **46** 37
- Mecerreyes D, Lee V, Hawker C J, Hedrick J L, Wursch A, Volksen W, Magbitang T, Huang E and Miller R D 2001 *Adv. Mater.* **13** 204
- Harth E, Van Horn B, Lee V Y, Germack D S, Gonzales C P, Miller R D and Hawker C J 2002 *J. Am. Chem. Soc.* **124** 8653
- Kumar K Y, Muralidhara H B, Nayaka Y A, Hanumanthappa H, Veena M S and Kumar S R K 2015 *Bull. Mater. Sci.* **38** 271
- Tan G X, Liao J W, Ning C Y and Zhang L 2012 *J. Appl. Polym. Sci.* **125** 3509
- Munoz-Bonilla A, van Herk A M and Heuts J P A 2010 *Polym. Chem.* **1** 624
- Lopez-Leon T, Ortega-Vinuesa J L, Bastos-Gonzalez D and Elaissari A 2006 *J. Phys. Chem. B* **110** 4629
- Liu J, Wang H T, Cheng S A and Chan K Y 2004 *Chem. Commun.* 728
- Gonzalez R, Figueroa J M and Gonzalez H 2002 *Eur. Polym. J.* **38** 287

25. Wang Z, Lu Z, Huang X, Xue R and Chen L 1998 *Carbon* **36** 51
26. Haas I, Shanmugam S and Gedanken A 2006 *J. Phys. Chem. B* **110** 16947
27. Choura M, Belgacem N M and Gandini A 1996 *Macromolecules* **29** 3839
28. Barr J B and Wallon S B 1971 *J. Appl. Polym. Sci.* **15** 1079
29. Fawcett A H and Dadamba W 1982 *Makromol. Chem.* **183** 2799
30. Principe M, Ortiz P and Martinez R 1999 *Polym. Int.* **48** 637
31. Chuang I S, Maciel G E and Myers G E 1984 *Macromolecules* **17** 1087
32. Paine A J, Luymes W and McNulty J 1990 *Macromolecules* **23** 3104
33. Lee J W, Ha J U, Choe S, Lee C S and Shim S E 2006 *J. Colloid Interface Sci.* **298** 663
34. Ye Q, He W D, Ge X W, Jia H T, Liu H R and Zhang Z C 2002 *J. Appl. Polym. Sci.* **86** 2567
35. Yan Y, Yang H F, Zhang F Q, Tu B and Zhao D Y 2006 *Small* **2** 517
36. Sun X M, Liu J F and Li Y D 2006 *Chem. Eur. J.* **12** 2039